



Restricted and Shared Patterns of TCR β -chain Gene Expression in Silicone Breast Implant Capsules and Remote Sites of Tissue Inflammation

Terrance P. O'Hanlon¹, Oliver J. Lawless², William E. Katzin³, Lu-Jean Feng⁴ and Frederick W. Miller¹

¹Laboratory of Molecular and Developmental Immunology, Center for Biologics Evaluation and Research, Food and Drug Administration, Bethesda, MD 20892, USA

²Center for Arthritis, Immunology, and Environmental Disorders, Olney, MD 20832, USA

³Department of Pathology and

⁴Division of Plastic Surgery, Mt. Sinai Medical Center, and Case Western Reserve University School of Medicine, Cleveland, OH 44106, USA

Received 4 February 2000

Accepted 10 March 2000

Key words: human, inflammation, silicone, T-cell receptors

Silicone breast implants (SBI) induce formation of a periprosthetic, often inflammatory, fibrovascular neo-tissue called a capsule. Histopathology of explanted capsules varies from densely fibrotic, acellular specimens to those showing intense inflammation with activated macrophages, multinucleated giant cells, and lymphocytic infiltrates. It has been proposed that capsule-infiltrating lymphocytes comprise a secondary, bystander component of an otherwise benign foreign body response in women with SBIs. In symptomatic women with SBIs, however, the relationship of capsular inflammation to inflammation in other remote tissues remains unclear. In the present study, we utilized a combination of TCR β -chain CDR3 spectratyping and DNA sequence analysis to assess the clonal heterogeneity of T cells infiltrating SBI capsules and remote, inflammatory tissues. TCR CDR3 fragment analysis of 22 distinct beta variable (BV) gene families revealed heterogeneous patterns of T cell infiltration in patients' capsules. In some cases, however, TCR BV transcripts exhibiting restricted clonality with shared CDR3 lengths were detected in left and right SBI capsules and other inflammatory tissues. DNA sequence analysis of shared, size-restricted CDR3 fragments confirmed that certain TCR BV transcripts isolated from left and right SBI capsules and multiple, extracapsular tissues had identical amino acid sequences within the CDR3 antigen binding domain. These data suggest that shared, antigen-driven T cell responses may contribute to chronic inflammation in SBI capsules as well as systemic sites of tissue injury.

© 2000 Academic Press

Introduction

It is estimated that since the early 1960s approximately 1–2 million women have received silicone breast implants (SBIs) in the United States for reconstructive mammoplasty and cosmetic augmentation [1]. Despite this long history of clinical use, little is known about the nature and determinants of human immune responses induced by SBIs. In 1992, the U.S. Food and Drug Administration requested a voluntary moratorium on the use of SBIs following increased reports of SBI failures (e.g. leakage and rupture) and multiple cases of atypical connective tissue disease developing in some women with SBIs [2–4]. Since that time, considerable debate has ensued regarding the safety of SBIs particularly in regard to the immunopathologic consequences of silicone gel exposure. Although several epidemiological studies failed to

detect an increased risk for the development of common connective tissue diseases after SBIs, these investigations were limited in their ability to assess risks for the development of rare or atypical autoimmune syndromes due to the size of the studies and various design and methodological limitations [4–6].

SBIs, when implanted in the body, induce formation of a periprosthetic neo-tissue called a capsule. The development of this fibrovascular tissue is a dynamic process and often results in the formation of an organized and multilayered structure [5, 7]. At the surface of the SBI, a capsule consists of a layer of vacuolated phagocytic cells, known as a pseudo-synovium, overlaid by a vascular connective tissue often containing inflammatory cells [1, 5, 8–11]. These inflammatory cells include activated macrophages, multinucleated giant cells, and T and B lymphocytes [5, 11–13]. In some capsules, lymphocytes are seen surrounding tissue vacuoles and macrophages containing a highly refractile, non-polarizable foreign material morphologically and chemically consistent with silicone [9, 14, 15].

Correspondence to: Terrance P. O'Hanlon, Food and Drug Administration, Bldg. 29B, Rm. 2G11, HFM-561, 8800 Rockville Pike, Bethesda, Maryland 20892, USA. Fax: 1–301 827 0852.

Several lines of indirect evidence suggest that SBIs induce immune responses when implanted in humans and animals. These data include the presence of chronic lymphocytic infiltrates in SBI capsules [5, 11–13], the adjuvant activity of some silicones in animals [16], the development of humoral and cellular immune abnormalities following SBIs [5, 17–25], T cell stimulatory responses induced by silicones *in vitro* [5, 21, 22], and case reports describing connective tissue diseases in SBI recipients, some of which resolve following explanation [3, 6, 26–29]. Based upon studies in humans and animals, it is clear that silicone gel diffuses from SBIs at the site of implantation and may migrate to multiple, distant organs and tissues [1, 5–7, 10, 30, 31]. What is uncertain, however, is whether any immunological relationship exists between local inflammatory responses detected in SBI capsules and systemic sites of tissue injury.

T lymphocytes are thought to contribute to pathology in many chronic inflammatory diseases [32, 33]. In SBI capsules, T cells comprise the majority of lymphocytes detected among inflammatory cells [11–13]. Whether capsule-infiltrating T cells accumulate in response to local antigenic stimulation or represent a secondary, bystander component of inflammation is unknown. Multiple studies of T cell-mediated autoimmune disease in humans and animals have focused on the nature of TCR gene expression at sites of inflammation [32–41]. T cells express a diverse class of clonotypic TCRs. Among $\alpha\beta$ cells, cell-surface TCRs are encoded by functionally rearranged V, D (β -chain only), J, and C gene segments. The recognition of antigens by $\alpha\beta$ -TCRs is mediated, in part, by complementarity determining regions (CDR3) spanning the V(D)J junctions of rearranged TCR genes [42]. CDR3 sequence diversity is enhanced further by the addition and deletion of random nucleotides (designated N-regions) positioned between V, D, and J gene segments. Specific antigens are often recognized by T cells expressing a limited or restricted number of TCR V(D)J sequence combinations [32–35, 43, 44]. Such biases reflect strong selective pressures for specific amino acid sequences within the CDR3 antigen binding domain [42]. Consistent with these observations, studies of experimentally-induced and spontaneous forms of autoimmune disease have identified restricted and shared patterns of TCR gene expression among pathogenic T cells [32–37, 39–42, 44].

Molecular studies of TCR gene expression have proven useful in identifying antigen-specific T cells in complex inflammatory infiltrates [32, 33, 36]. In a previous study, we examined patterns of TCR gene expression in 20 capsules from SBI recipients using a low resolution V gene family-specific RT-PCR assay [13]. These data indicated that similar patterns of TCR V gene expression were conserved between left and right SBI capsules in some implant recipients irrespective of clinical status. In the present study, we extend these findings utilizing a combination of high resolution TCR CDR3 spectratyping and direct DNA sequence analysis to assess the clonal heterogeneity of

T cells found infiltrating SBI capsules and remote sites of tissue inflammation.

Materials and Methods

Patients and clinical material

The collection and analysis of clinical materials were done after obtaining informed patient consent for enrollment in IRB-approved clinical protocols. Clinical specimens, including blood samples and concurrent tissue biopsies were collected at the time of the surgical procedures. Portions of tissues were rapidly frozen on dry ice and stored at -80°C until processing. Three patients were studied extensively in this investigation. Patient #1 is a 46-year-old woman with a 20-year history of SBIs for augmentation (HLA DRB1*0403, 1501; DQA1*0102, 0301). She was diagnosed with rheumatoid factor-negative rheumatoid arthritis prior to SBI implantation, but later developed a syndrome consisting of severe systemic vasculitis, peripheral neuropathy, and worsening of her arthritis post-implantation. A bilateral explant was performed in response to her clinical status and a unilateral implant rupture. Patient #2 is a 41-year-old woman with a 13-year history of SBIs for augmentation (HLA DRB1* 0101, 1301; DQA1*0101, 0103). Post-implantation, she was diagnosed with an atypical connective tissue disease consisting of diffuse arthralgias, myalgias, chronic fatigue, and axillary lymphadenopathy. Explantation was performed in response to concerns about her worsening clinical status. Patient #3 is a 54-year-old woman with a 14-year history of SBIs placed during reconstructive mammoplasty after mastectomy for breast cancer (HLA DRB1*0403, 1501; DQA1*0102, 0301). She developed an undifferentiated connective tissue disease consisting of arthralgias, myalgias, chronic fatigue, diffuse rashes, systemic vasculitis, and a monoclonal gammopathy of undetermined significance post-implantation. Unilateral device rupture was noted upon explantation.

Immunohistology

Portions of tissues obtained at surgery were formalin-fixed and paraffin-embedded for immunocytochemical analysis. Serial sections (five μm) from each specimen were deparaffinized and subjected to microwave treatment [45, 46]. Processed sections were incubated with primary antibodies (CD3 and CD4, Novacastra, Newcastle, UK; CD8 and CD45RO, Dako, Carpinteria, CA, USA) and subsequently localized using a modified avidin-biotin immunoperoxidase method (Vector Laboratories, Burlingame, CA, USA).

RNA extraction, cDNA synthesis, and PCR amplification

Total RNA was isolated from tissues (200 mg/capsule or 50 mg/lymph node, muscle, or skin biopsy) and

PBLs by homogenization followed by Trizol extraction (Gibco BRL, Gaithersburg, MD, USA). Purified RNA (5.0 µg) was utilized for random-primed cDNA synthesis using the GeneAmp RT-PCR protocol (Perkin Elmer, Norwalk, CT, USA). The cDNA product was used for individual PCR amplifications (100 ng RNA equivalents per 25 µl reaction) with one of 23 distinct 5' TCR beta-variable (BV) gene-family-specific primers and a shared 6FAM-labeled 3' TCR BC gene primer according to established methods and nomenclature [47–49]. TCR BV10 and BV19 pseudogene families were excluded from the analysis [50]. PCR was performed for 35 (PBL) or 40 (tissues) cycles using a two-step cycling program (denaturation, 95°C for 15 s; annealing, 55°C for 20 s). Control amplifications for μ -actin (5' primer, caccttctacaatgagctgcg; 3' primer, tgcttgctgatccacatctgc) were performed from each sample to confirm cDNA integrity and assure that approximately equivalent amounts of cDNAs were utilized for TCR analysis (data not shown). Sensitivity of the TCR BV spectratyping assay was determined by spiking variable numbers of human Jurkat T cells (10^2 – 10^6) into serial sections of a non-inflammatory SBI capsule prior to homogenization and RNA extraction. Based upon the assay conditions described above, the limit of TCR BV transcript detection was estimated between 10^2 – 10^3 T cells (data not shown).

TCR spectratyping, DNA cloning, and sequence analysis

TCR BV gene family-specific amplification products were size-fractionated in 4.75% denaturing polyacrylamide gels and scanned directly with a fluorimager model SI (Molecular Dynamics, Sunnyvale, CA, USA) [48]. Patients' PBL and tissue samples were analysed in parallel to ensure assay integrity and confirm that tissue-derived PCR products corresponded with the predicted sizes of TCR BV gene amplification products detected in peripheral blood. For cloning analysis, TCR BV amplification products of interest were size-fractionated as described above, excised from polyacrylamide gels, crushed in 500 µl of 50 mM TRIS (pH 8.0), and incubated overnight at +4°C. Eluted DNA (5 µl) was subsequently re-amplified using corresponding 5' TCR BV primers and a nested 3' TCR BC primer (5'gcgacctcgggtgggaacac3') for 20 cycles as described above. The resulting amplification products were size-fractionated in 2% agarose gels and purified using the Qiaex gel extraction protocol (Qiagen Inc., Chatsworth, CA, USA). Eluted DNA was ligated within the pCR 2.1 T/A cloning vector (Invitrogen, Inc., San Diego, CA, USA) and used to transform bacterial cells as described by the manufacturer. Independent recombinants, identified by antibiotic selection and β -galactosidase colorimetric assay, were grown overnight in mini-culture and screened subsequently by DNA dot blot hybridization using a TCR BC horseradish peroxidase-conjugated oligonucleotide probe and chemiluminescent detection as

described previously [51]. Plasmid DNA, purified from positively-hybridizing bacterial lysates, was used as template for fluorescent dye terminator DNA sequencing with an ABI Model 377 automated sequencer (PE Applied Biosystems, Foster City, CA, USA). Nucleic acid and protein sequence comparisons were performed using PCGENE sequence analysis software (Intelligenetics, Mountain View, CA, USA).

Results

Immunohistopathology

We have evaluated 46 capsules to date and determined that their histopathology varied from nearly acellular, densely fibrotic capsules to those showing intense inflammation ([11, 13] and unpublished results). Capsular infiltrates were generally comprised of activated macrophages, multinucleated giant cells, and variable numbers of T and B lymphocytes. In some instances, lymphocytes were seen surrounding tissue vacuoles and macrophages containing a highly refractile, foreign material consistent with that observed for silicone [14]. In a representative analysis, serial sections obtained from an inflammatory SBI capsule illustrate the orientation of CD4+ and CD8+ T cells co-expressing CD45RO, an anamnestic marker of T cell activation, around tissue vacuoles containing a material morphologically consistent with silicone (Figure 1). The frequent detection of activated T cells found infiltrating SBI capsules prompted our examination of TCR gene expression for evidence of antigen-driven T cell responses.

TCR BV spectratype analysis

TCR spectratyping is a rapid and sensitive means of evaluating the clonal composition of T cells expressing a common V gene family based upon variations in the lengths of CDR3 antigen binding domains [48]. To examine the heterogeneity of T cell clones found infiltrating patients' tissues, we analysed CDR3 spectratypes for each of 22 distinct TCR BV gene families. We first validated the TCR BV CDR3 spectratyping assay by analysing a polyclonal population of T cells isolated from PBL of a healthy donor (Figure 2). The resulting fluorograph permits the discrimination of multiple, functionally rearranged TCR BV gene-family-specific transcripts. Variations in the lengths of intervening CDR3 regions produce the characteristic 'ladder' of bands (CDR3 spectratype) detected for each of the BV gene families. Adjacent bands in a given ladder vary by increments of three nucleotides (corresponding to one amino acid) within the CDR3 antigen binding domain. This representative analysis illustrates the heterogeneity of TCR BV gene expression consistent with the polyclonal composition of T cells in the peripheral blood.

Similar analyses of RNA isolated from 34 SBI capsules using a combination of low and high resolution

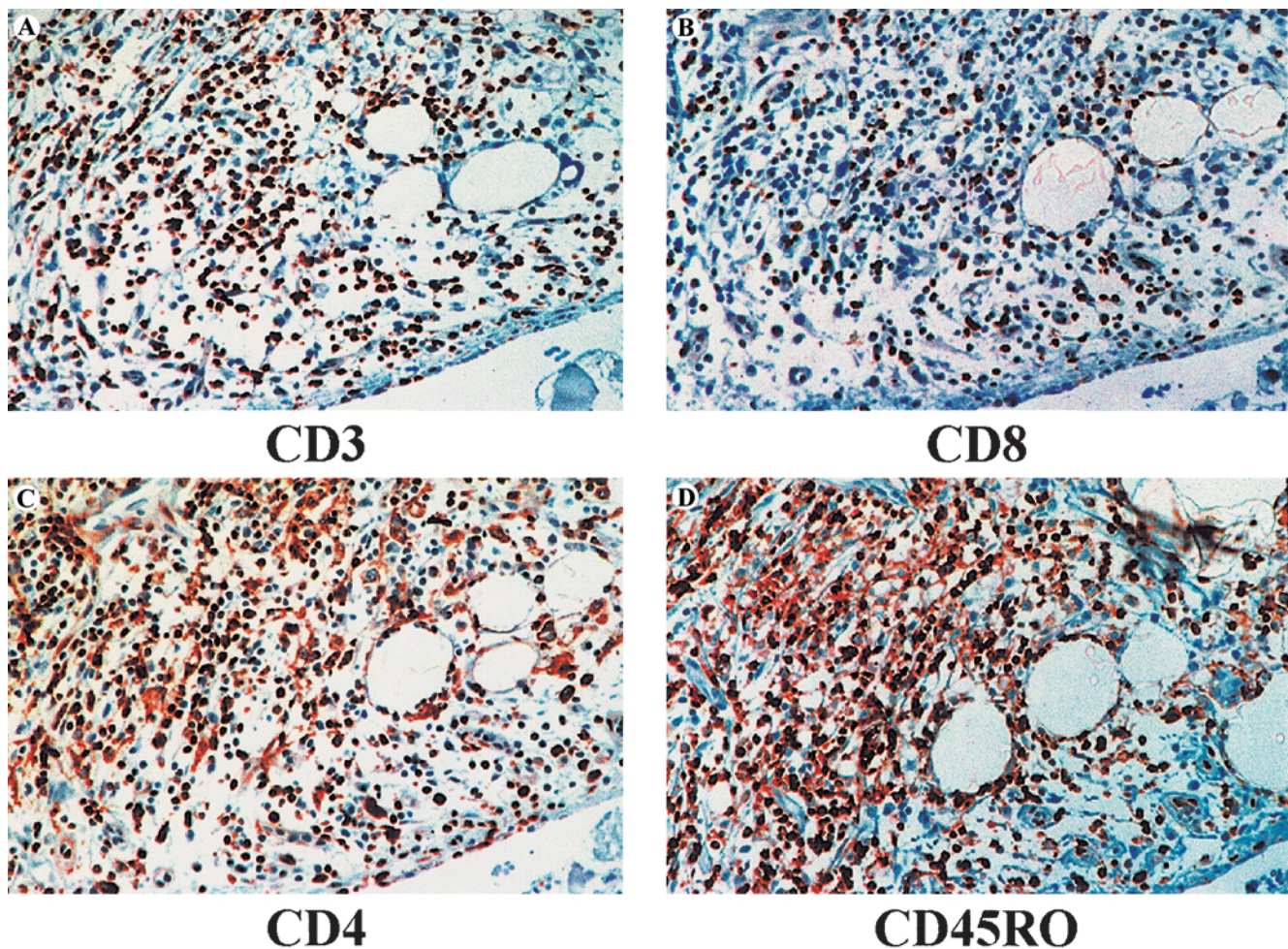


Figure 1. Immunohistologic evaluation of T cell infiltrates in SBI capsules. Shown is a representative immunocytochemical analysis of serial sections of a SBI capsule stained using monoclonal antibodies reactive with CD3 (A), CD8 (B), CD4 (C), and CD45RO (D) as described in Materials and Methods (original magnification 50 \times). T cells were often seen in association with tissue vacuoles containing a highly refractile, foreign material morphologically consistent with silicone [14].

TCR typing assays revealed that capsular T cell infiltrates varied widely and ranged from an absence of detectable TCR gene expression to the detection of multiple TCR V gene families ([13] and data not shown). While the number and identity of TCR V gene families detected varied considerably among capsules, in some instances, shared and restricted patterns of V gene expression were detected in both the left and right capsules from individuals independent of their clinical status (i.e., symptomatic and asymptomatic patients). A representative TCR BV CDR3 spectratype analysis of RNA from PBL, left capsule, and right capsule from patient #1 is illustrated in Figure 3. As expected, a polyclonal pattern of TCR BV gene expression was detected in PBL (Figure 3, lane 1). In contrast, a more restricted or oligoclonal profile of TCR BV gene expression was detected in the patient's left and right capsules (Figure 3, lanes 2 and 3, respectively). While dissimilar patterns of restricted TCR gene expression were detected for the majority of BV genes surveyed, in some cases, amplification products with identical CDR3 lengths were detected between left and right capsules (e.g., Figure 3, BV3 and BV13). These data suggested that an antigen-

driven clonal expansion might possibly account for the detection of identically sized TCR transcripts in both left and right SBI capsules.

To further examine the potential for antigen-driven T cell responses shared among inflammatory tissues, we focused our analysis on three SBI patients from whom, in two cases, multiple biopsies of clinically affected tissues were available. Patients' PBL, left and right SBI capsules, and remote tissue biopsies, when available, were analysed by the TCR BV CDR3 spectratyping assay illustrated in Figure 3. A comprehensive alignment of BV CDR3 spectratype data obtained from each patient's tissues was conducted in an effort to identify size-restricted TCR transcripts shared among multiple, physically remote sites of inflammation (data not shown). Two TCR BV gene families with transcripts exhibiting shared CDR3 lengths among multiple inflammatory tissues were arbitrarily chosen from each patient for further analysis (Figure 4). For patient #1, a 162 bp TCR BV13 amplification product was detected from both left and right SBI capsules (LC and RC, respectively), skeletal muscle (SM), and three independent skin biopsies (SK1, chest; SK2, vasculitic lesion-right hand; SK3, vasculitic lesion-left hand)

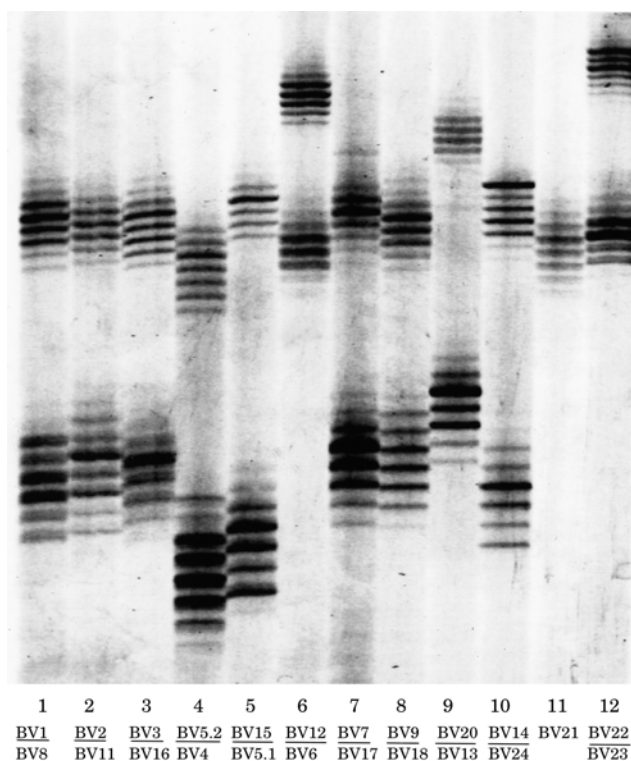


Figure 2. TCR BV gene family-specific RT-PCR analysis of PBL from a healthy donor. TCR spectratype analysis of peripheral blood illustrates the range of CDR3 length variation for each of the 22 BV gene families amplified from a polyclonal T cell population. Variations in CDR3 length produce the characteristic 'ladder' of bands detected for each of the TCR BV gene families. Adjacent bands in a given ladder vary by three nucleotide increments corresponding to single amino acid length differences within the CDR3 antigen binding domain. The identities of individual TCR BV gene families are listed below the fluorograph. With the exception of BV21, note that two sets of TCR BV gene family amplification products were size-fractionated in each lane of the gel (e.g., in Lane 1, BV1/BV8 denotes that the TCR BV1 gene family spectratype is positioned above the TCR BV8 gene family spectratype). The size of the TCR amplification products detected correspond with those predicted for the respective BV gene families (range, 140–250 bp).

(Figure 4A, left panel). A TCR BV3 fragment (199 bp) shared among both SBI capsules, skeletal muscle, and one skin biopsy (SK2) was also detected from this same patient, (Figure 4A, right panel). Similarly, TCRs bearing identical CDR3 lengths were detected in capsules and two axillary lymph nodes (LN1 and LN2) from patient #2 (BV18, 149 bp and BV24, 149 bp) and from both the left and right capsules of patient #3 (BV14, 197 bp; BV21, 196 bp) (Figure 4B & C, respectively). While intriguing, the detection of common, size-restricted TCR transcripts shared among multiple tissues does not confirm that identical or similar T cell clones are present among these tissue infiltrates (i.e., TCRs with identically sized CDR3 regions may have unrelated amino acid sequences). To resolve this question, we next determined the clonal identity of these

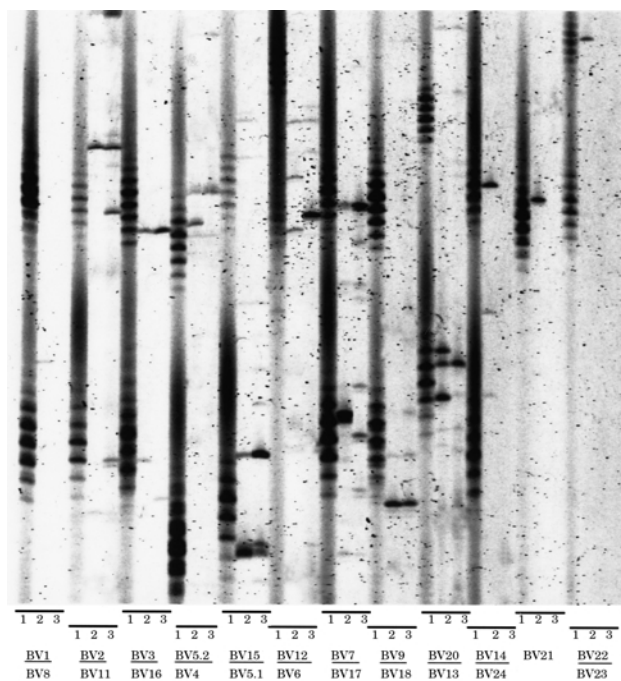


Figure 3. Representative TCR BV spectratype analysis of SBI capsules. Shown are results illustrating the range and variability of TCR BV gene expression detected in the PBL (lane 1), left capsule (lane 2), and right capsule (lane 3) from patient #1 described in Materials and Methods. Parallel analysis of patient's PBL served as a molecular size standard and positive control for the detection of the 22 TCR BV gene families surveyed (range, 140–250 bp). The identity of individual TCR BV gene families is listed below the fluorograph. Note that two sets of TCR BV gene family amplification products were size-fractionated in each lane of the gel (except BV21) as described in Figure 2.

shared transcripts by direct DNA sequence analysis of the CDR3 antigen binding region.

Assessment of T cell clonality by TCR sequence analysis

To assess T cell clonality, we gel-purified, cloned, and determined the amino acid sequences of the TCR BV amplification products shared among multiple tissues in these patients. As shown in Figure 5A, an amino acid sequence alignment of BV13 transcripts (162 bp) isolated from patient #1 revealed a heterogeneous pattern of TCR gene expression among tissues. As expected, multiple, unrelated clonotypes (i.e., independently rearranged TCR genes) sharing identical CDR3 lengths were detected among PBL reflecting the polyclonal nature of circulating T lymphocytes. A polyclonal pattern of BV13 gene expression was also detected among T cells infiltrating a vasculitic skin lesion (SK3). A more restricted or oligoclonal pattern of BV13 gene expression was detected among the remaining tissues (LC, RC, SM, SK1, and SK2). There was no obvious amino acid sequence similarity within the CDR3 antigen binding domain detected among these BV13 tissue-infiltrating T cells. In contrast, a similar analysis of BV3 transcripts (199 bp) isolated

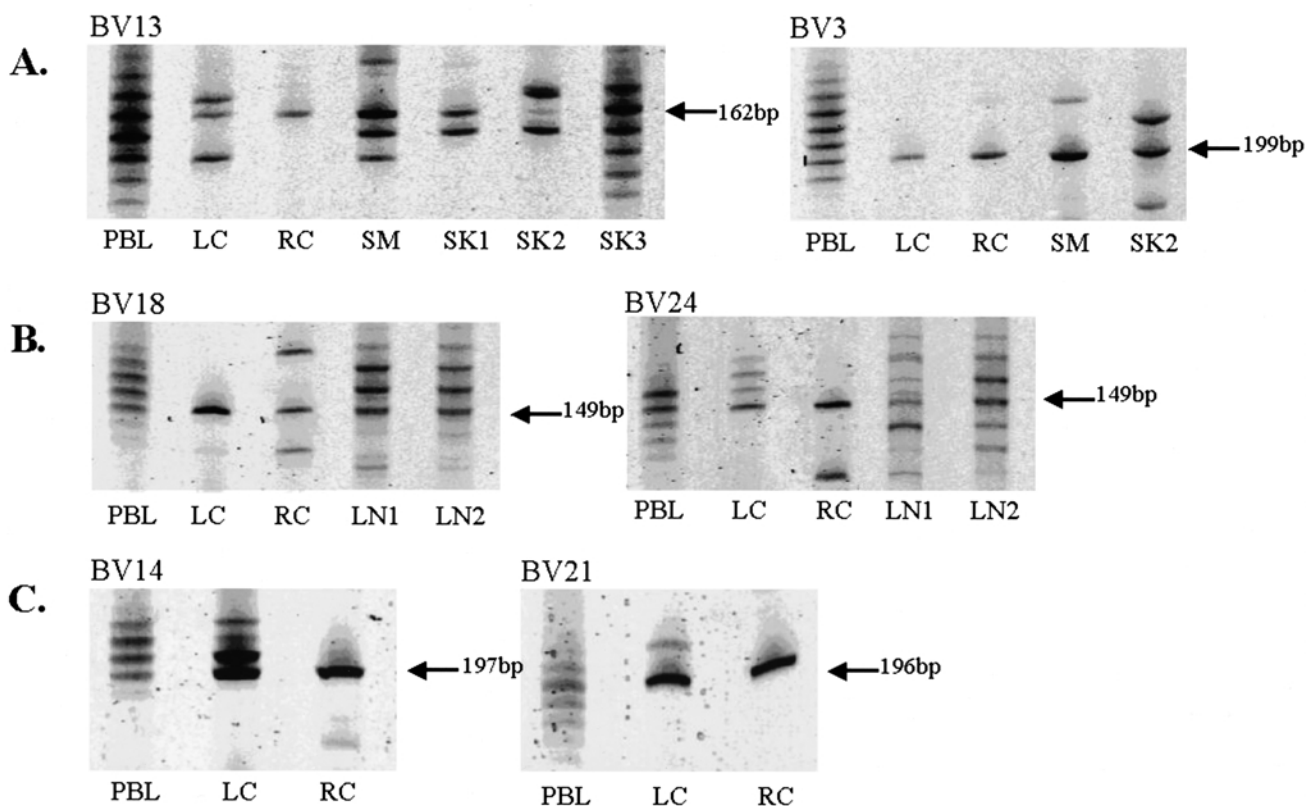


Figure 4. TCR BV spectratype analysis of SBI capsules and remote, inflammatory tissues from patients with connective tissue disease. Shown are selected spectratypes of TCR BV gene families from which transcripts with identical CDR3 lengths were detected among left and right SBI capsules and, in some cases, remote, inflammatory tissues. A, Spectratype alignments of TCR BV13 (left panel) and BV3 (right panel) gene family amplification products from patient #1 are shown. Arrows indicate TCR transcripts of identical size (BV13, 162 bp and BV3, 199 bp) that are shared among multiple inflammatory tissues (LC, left capsule; RC, right capsule; SM, skeletal muscle; SK1, skin biopsy from the chest; SK2, vasculitic skin lesion from the right hand; SK3, vasculitic skin lesion from the left hand). The 199 bp BV3 transcript was not detected in tissues SK1 and SK3 (data not shown). B, TCR spectratype alignment shows BV18 (left panel) and BV24 (right panel) amplification products from which transcripts of identical size (149 bp) were detected in the LC, RC, and two axillary lymph nodes (designated LN1 and LN2) from patient #2. C, For patient #3, a similar alignment of TCR BV14 (left panel) and BV21 (right panel) spectratypes shows identically sized transcripts (197 bp and 196 bp, respectively) shared between left and right SBI capsules.

from the same patient revealed that identical T cell clones were present among multiple, remote inflammatory tissues (Figure 5B). Two BV3 clones (CDR3 sequences: RYVA/GEL and EGV/QETQ) were detected among the otherwise polyclonal capsular infiltrates and the oligoclonal infiltrate seen in skeletal muscle. Of interest, the clonotype defined by the EGV/QETQ sequence was also detected among circulating T cells. One of the shared TCR clonotypes (RYVA/GEL) represented the predominant transcript detected among BV3 T cells infiltrating skeletal muscle and a vasculitic skin lesion (SK2).

A similar analysis of CDR3 amino acid sequences of TCR BV18 and BV24 transcripts (149 bp) was performed in specimens from patient #2 (Figure 6A, left and right panels, respectively). While a single BV24 clonotype was detected from each of the SBI capsules, these clones lacked amino acid sequence identity with one another and with BV24 clones isolated from axillary lymph nodes (LN1 and LN2). In contrast, an identical BV18 clone (CDR3 sequence: PGPTH/EQ) was detected in both left and right capsules as well as within a more polyclonal lymph node population

(LN1). Figure 6B summarizes an analysis of BV14 (197 bp) and BV21 (196 bp) capsular-infiltrating T cells from patient #3 (left and right panels, respectively). In this case, identical BV14 clones (CDR3 sequence: PTSED/EQ) represented the predominant clonotypes shared between left and right SBI capsules. Two distinct BV14 clonotypes (STVAG/EQ and STAAG/EQ) that differed by only a single, conservative amino acid substitution (V/A) within the CDR3 domain were also detected in the right capsule (Figure 6C). No apparent amino acid sequence similarities were noted among BV21 capsular-infiltrating T cells from this patient (Figure 6B, right panel).

Discussion

T lymphocytes are a prominent feature of inflammatory infiltrates in some SBI capsules [11–13]. When present, activated CD4+ and CD8+ T cells are often seen surrounding tissue vacuoles and macrophages containing a highly refractile, foreign material

A.					B.					
	BV13	N-D-N	BJ	FREQ		BV3	N-D-N	BJ	FREQ	
PBL	CASS	SDSGA	NYGYTFG (1S2)	1/10	PBL	CASS	P*Q	NEQFFG (2S1)	1/10	
	CASS	DRADSGH	EQFFG (2S1)	1/10		CASS	VIL	DTQYFG (2S3)	1/10	
	CAS	RSRTEVP	DTQYFG (2S3)	1/10		CAS	EGV	QETQYFG (2S5)	3/10	
	CASS	YSMAGP	YEQYFG (2S7)	1/10		CAS	LIY	QETQYFG (2S5)	1/10	
	CAS	LTPTPPRG	EQYFG (2S7)	1/10		CASS	TTL	YEQYFG (2S7)	1/10	
	CASS	VQGLS	SYEQYFG (2S7)	1/10		CASS	STWR	EQYFG (2S7)	1/10	
	CASS	YAPGGN	YEQYFG (2S7)	2/10		CAS	NKWQ	YEQYFG (2S7)	1/10	
	CASS	YGTGFF	YEQYFG (2S7)	1/10		CAS	RPH	SYEQYFG (2S7)	1/10	
	CAS	TAHTGGT	YEQYFG (2S7)	1/10		LC	CAS	RTDRLA	AFFG (1S1)	1/10
	LC	CASS	PTSGFD	NEQFFG (2S1)			10/10	CAS	RPMNP	EAFFG (1S1)
RC		CASS	ETGGA	YNEQFFG (2S1)	10/10		CAS	DES	NTEAFFG (1S1)	1/10
	SM	CASS	SGDRNSLG	AFFG (1S1)	1/10		CASS	TG	NYGYTFG (1S2)	1/10
CASS		RAWG	SNQPQHFG (1S5)	6/10	CAS		GTA	NEKLFFG (1S4)	1/10	
CASS		PTGTD	SYEQYFG (2S7)	3/10	CAS		RYVA	GELFFG (2S2)	1/10	
SK1	CASS	NSWT	NTGELFFG (2S2)	10/10	CAS		EGV	QETQYFG (2S5)	1/10	
	SK2	CAS	TFDGM	SNQPQHFG (1S5)	10/10		CASS	SKAG	TQYFG (2S5)	1/10
SK3		CASS	YRREGVG	GYTFG (1S2)	1/10		CASS	STWR	EQYFG (2S7)	1/10
	CASS	FRNGV	NEKLFFG (1S4)	2/10	CASS		DGA	YEQYFG (2S7)	1/10	
	CASS	GTGGSG	QPQHFG (1S5)	1/10	RC	CASS	SNE	QPQHFG (1S5)	1/10	
	CASS	YSFKG	YNEQFFG (2S1)	1/10		CASS	TT	NQPQHFG (1S5)	1/10	
	CAS	RGLAVKG	DTQYFG (2S3)	1/10	CASS	TGD	SPLHFG (1S2)	1/10		
	CASS	FTLPY	TDTQYFG (2S3)	1/10	CAS	RYVA	GELFFG (2S2)	3/10		
	CAS	RNADWDR	ETQYFG (2S5)	1/10	CAS	EGV	QETQYFG (2S5)	3/10		
	CASS	YPI	SGANVLTFG (2S6)	1/10	CASS	LVY	YEQYFG (2S7)	1/10		
	CASS	YREPGID	EQYFG (2S7)	1/10	SM	CASS	FNRRER	QFFG (2S1)	1/10	
						CAS	RYVA	GELFFG (2S2)	7/10	
				CAS	EGV	QETQYFG (2S5)	2/10			
				SK2	CAS	RYVA	GELFFG (2S2)	10/10		

Figure 5. TCR CDR3 sequence analysis of tissue-infiltrating T cells from patient #1. Shown are the amino acid sequence alignments (single letter code) of the 162 bp BV13 (panel A) and 199 bp BV3 (panel B) gene amplification products designated in Figure 4. The junctional sequences (VDJ) of distinct TCR clonotypes (i.e., independently rearranged TCR genes) identified from each of the tissues analysed are shown (abbreviations per Figure 4). The identity of germline TCR BJ gene family members is indicated in parentheses to the right of the BJ sequences. The frequency of detection of each TCR clonotype (i.e., the number of identical TCR clonotypes identified per 10 independent recombinants analysed) is indicated to the right of the alignment. Identical TCR clonotypes detected among multiple inflammatory tissues are highlighted in bold type. The approximate boundaries of the TCR antigen binding domain (CDR3) are shown below the alignment.

morphologically consistent with silicone (e.g. see Figure 1). It remains unclear, however, whether capsule-infiltrating T cells are antigen-driven or if they comprise a secondary, non-specific component of an otherwise benign foreign body response. We hypothesized that among capsule-infiltrating T cells, a subpopulation of antigen-driven cells may contribute to chronic inflammation in these and possibly remote sites of tissue injury.

It has been demonstrated in both humans and animal models that antigen-reactive, pathogenic T cells comprise a minority of infiltrating T cells in chronic inflammatory lesions [33, 34]. In these cases, the majority of T cells in chronic lesions likely represent secondary, bystander cells attracted by proinflammatory migratory signals [33, 52]. It is clear that the TCR CDR3 domain serves as a primary specificity determinant for T cell antigen recognition [42]. In fact, the detection of T cells expressing restricted and

conserved TCR CDR3 sequence rearrangements is considered a hallmark of antigenic reactivity. For these reasons, we chose the TCR CDR3 spectratyping technique as a means of screening heterogeneous populations of tissue-infiltrating T cells to assess if T cell clones were shared among multiple pathologic lesions [40, 48].

In an effort to identify putatively antigen-reactive T cells, we determined the pattern of TCR BV gene expression in SBI capsules and remote inflammatory tissues using a combination of CDR3 spectratyping and DNA sequence analysis. Overall, the number and identity of TCR BV gene families detected varied considerably among tissues and patients ([13] and data not shown). By comparing CDR3 size-fractionated BV gene transcripts (i.e., spectratypes), we identified common, size-restricted transcripts shared among multiple inflammatory tissues (Figures 3 & 4). DNA sequence analysis confirmed that, at least

A.

	BV18	N-D-N	BJ	FREQ		BV24	N-D-N	BJ	FREQ
LC	CASS	PGPTH	EQYFG (2S7)	10/10	LC	CAT	RPGTGDS	YGTYFG (1S2)	10/10
RC	CASS	PGPTH	EQYFG (2S7)	10/10	RC	CATS	RDGTVGNTV	YFG (1S3)	10/10
LN1	CASS	QGG	NTEAFFG (1S1)	1/10	LN1	CATS	RAGGSL	ETQYFG (2S5)	3/10
	CASS	PHLDS	EAFFG (1S1)	1/10		CATS	RDRVN	QETQYFG (2S5)	7/10
	CASS	PEA	NYGYTFG (1S2)	1/10	LN2	CAT	TTPRSG	NTEAFFG (1S1)	1/10
	CASS	PY	SNQPQHFG (1S5)	5/10		CATS	REGQL	TGELFFG (2S2)	1/10
	CASS	PGPTH	EQYFG (2S7)	1/10		CATS	RDGDR	TDTQYFG (2S3)	1/10
	CASS	PNQY	YEQYFG (2S7)	1/10	CATS	RDAV	AKNIQYFG (2S4)	1/10	
LN2	CASS	RKDD	TEAFFG (1S1)	2/10	CATS	RDGGL	QETQYFG (2S5)	1/10	
	CASS	QGRG	TEAFFG (1S1)	1/10	CATS	RGEAGGGS	QYFG (2S5)	1/10	
	CASS	PTREA	EAFFG (1S1)	2/10	CATS	SEGGRN	NVLTFG (2S6)	1/10	
	CASS	PRPVG	GYTFG (1S2)	1/10	CATS	SLQGPQG	EQYFG (2S7)	1/10	
	CASS	PER	NYGYTFG (1S2)	2/10	CATS	REPHTVN	EQYFG (2S7)	2/10	
	CASS	QASSY	EQFFG (2S1)	1/10	CDR3				
	CASS	PPTA	DTQYFG (2S3)	1/10					
	CDR3								

B.

	BV14	N-D-N	BJ	FREQ		BV21	N-D-N	BJ	FREQ
LC	CASS	PTSED	EQFFG (2S1)	10/10	LC	CASS	FWAGS	QETQYFG (2S5)	8/10
RC	CASS	PTSED	EQFFG (2S1)	4/10	RC	CASS	PKGTV	QETQYFG (2S5)	2/10
	CASS	STVAG	EQYFG (2S7)	3/10		CASS	SSVLAKS	EQYFG (2S7)	10/10
	CASS	STAAG	EQYFG (2S7)	3/10		CDR3			
CDR3									

C.

C	A	S	S	S	T	V	A	G	E	Q	Y	F	G
TGT	GCC	AGC	AGT	TCG	ACA	GTG	GCC	GGG	GAG	CAG	TAC	TTC	GGG
***	***	***	***	***	**	*	**	**	***	***	***	***	***
TGT	GCC	AGC	AGT	TCG	ACT	GCT	GCT	GGC	GAG	CAG	TAC	TTC	GGG
C	A	S	S	S	T	A	A	G	E	Q	Y	F	G

Figure 6. TCR CDR3 sequence analysis of tissue-infiltrating T cells from patient #2 and patient #3. A, Shown for patient #2 are the amino acid sequence alignments (single letter code) of the 149 bp BV18 (left panel) and BV24 (right panel) gene amplification products designated in Figure 4B. A similar amino acid sequence alignment of the 197 bp BV14 (left panel) and 196 bp BV21 (right panel) PCR products is shown for patient #3. The junctional sequences (VDJ) of distinct TCR clonotypes (i.e., independently rearranged TCR genes) identified from each of the tissues analysed are shown (abbreviations per Figure 4). The identity of germline TCR BJ gene family members is indicated in parentheses to the right of the BJ sequences. The frequency of detection of each TCR clonotype (i.e. the number of identical TCR clonotypes identified per 10 independent recombinants analysed) is indicated to the right of the alignment. Identical TCR clonotypes detected among multiple inflammatory tissues are highlighted in bold type. The approximate boundaries of the TCR antigen binding domain (CDR3) are shown below the alignment. TCR BV gene sequences from corresponding PBL samples were not determined. C, A nucleotide sequence alignment of two BV14 clonotypes (CDR3 sequences: STVAG/EQ and STAAG/EQ) identified from the right capsule of patient #3 is shown. Regions of nucleotide sequence identity are designated (*). Corresponding amino acid sequences are positioned above and below the respective nucleotide sequences. Amino acid sequence differences are highlighted in bold type.

in some cases, identical T cell clones are found at sites of local (i.e., left and right capsules) and remote inflammation (Figures 5 & 6). The most dramatic example was the detection of a unique TCR BV3 clone (RYVA/GEL) in both left and right SBI capsules, skeletal muscle, and a vasculitic skin lesion isolated from patient #1 (Figure 5). In contrast, a parallel analysis of BV13 clones isolated from the same patient's tissues failed to identify a shared clonotype(s). This distinction between the pattern of BV3

and BV13 gene expression emphasizes the importance of direct DNA sequence analysis of amplification products that are size-restricted on polyacrylamide gels. In one case, the BV13 clones identified likely represent bystander T cells which coincidentally share CDR3 lengths but not sequence, while the identical BV3 clones identified from multiple tissues appear to be selected and expanded by a common antigen(s). Interestingly, one or more identical T cell clones were detected in both left and right SBI capsules from each

of the three patients analysed (Figures 5 & 6). We did not, however, detect any TCR clones shared among different patients despite the fact that two patients expressed identical HLA DRB1 and DQA1 antigens (see Materials and Methods). Based upon the transcript detection limit of our assay (10^2 – 10^3 T cells as described in Materials and Methods), these data are consistent with the clonal expansion of a limited or restricted number of antigen-reactive T cells. Moreover, the detection of two, distinct TCR clonotypes (STVAG/EQ and STAAG/EQ) utilizing identical BV14 and BJ2S7 gene segments and differing by only a single, conservative amino acid substitution (V/A) within the CDR3 antigen binding domain (Figure 6C), is additional evidence for antigenic selection of capsule-infiltrating T cells. Taken together, these data suggest that the same antigen-reactive T cell clones are present in SBI capsular infiltrates and remote inflammatory tissues. These findings are consistent with the detection of identical TCR clonotypes at multiple sites of inflammation from patients with autoimmune diseases including multiple sclerosis, psoriasis, Sjogren's syndrome, and rheumatoid arthritis [35, 37, 39, 41].

The identification of an antigen responsible for initiating and/or promoting chronic inflammation in SBI capsules and possibly in remote tissues has remained elusive. It is well documented that silicone gel diffuses from implant devices (referred to as 'silicone bleed') and that SBIs rupture in a time-dependent manner [1, 10, 30, 53, 54]. In either case, it is not uncommon for the body to be exposed to free silicone gel for extended periods of time. Several investigators employing *in vitro* T cell stimulatory assays have suggested that some silicones or silicone-conjugates may themselves provide an antigenic stimulus [5, 21, 22]. Alternatively, the strong adjuvant properties of certain silicones may render some endogenous proteins immunogenic [7, 16, 25]. Kossovsky and Freiman proposed that silicone, being very hydrophobic, may act as a powerful denaturant of capsule-associated connective tissue proteins (e.g. collagen) [7]. Recognition of denatured protein antigens by T cells might possibly initiate a broadening T cell response to multiple, formerly non-immunogenic epitopes of endogenous proteins. This model of epitope or determinant spreading has been well documented for a number of T cell antigens in various experimental and human autoimmune diseases [55, 56]. In fact, the generation of abnormal humoral (i.e., autoantibody production) and cellular immune responses to connective tissue proteins has been associated with silicone implantation [19, 25, 57].

In the present study, we examined patterns of TCR gene expression from SBI patients including two from which multiple, concurrent inflammatory tissue biopsies were available. Ours is the first report documenting that a limited number of distinct TCR clonotypes, presumably expanded by an antigen-driven process, are shared among the inflammatory infiltrates in patients' capsules and, in some cases, remote inflammatory lesions. Unfortunately, the analysis of chronic inflammatory lesions from patients with established disease does not permit a determination of

when, where, or how these shared T cell clones arose. Moreover, our laboratory has previously documented shared patterns of TCR V gene expression among capsules from asymptomatic SBI recipients ([13] and unpublished results). Thus it is unclear whether the shared T cell clones identified in this study are the result of silicone exposure or an unrelated immune process or disease state [33, 52]. Nevertheless, the detection of identical T cell clones at multiple pathologic sites in the same patient suggests that a shared antigenic stimulus may contribute to chronic inflammation at these sites.

The basis for the variability in the degree of inflammation detected among the capsules from different SBI recipients remains unknown. It seems plausible, however, that subjects might vary in their sensitivity to silicone and that different individuals, defined by unique immunogenetics and environmental exposures, may experience diverse spectra of immunologic and clinical outcomes [58, 59]. Studies are on-going to determine the mechanisms that regulate SBI capsule formation and the pathophysiologic role of capsule-infiltrating T cells.

Acknowledgements

The authors wish to thank Drs Suzanne Epstein and Steven Bauer for their critical review of the manuscript. This work was supported in part by research funding provided by the CBER/FDA and the FDA Office of Woman's Health. The statements and opinions expressed herein are the private views of the authors and not necessarily those of the institutions they represent.

References

- Emery J.A., Spanier S.S., Kasnic G., Jr. Hardt N.S. 1994. The synovial structure of breast-implant-associated bursae. *Mod. Pathol.* **7**: 728–733
- Kessler D.A. 1992. The basis of the FDA's decision on breast implants. *N. Engl. J. Med.* **326**: 1713–1715
- Brown S.L., Parmentier C.M., Woo E.K., Vishnuvajjala R.L., Headrick M.L. 1998. Silicone gel breast implant adverse event reports to the Food and Drug Administration, 1984–1995. *Public Health Rep.* **113**: 535–543
- Brown S.L., Langone J.J., Brinton L.A. 1998. Silicone breast implants and autoimmune disease. *J. Am. Med. Womens. Assoc.* **53**: 21–4
- Shanklin D.R., Smalley D.L. 1998. The immunopathology of siliconosis. History, clinical presentation, and relation to silicosis and the chemistry of silicon and silicone. *Immunol. Res.* **18**: 125–173
- Yoshida S.H., Swan S., Teuber S.S., Gershwin M.E. 1995. Silicone breast implants: immunotoxic and epidemiologic issues. *Life Sci.* **56**: 1299–1310
- Kossovsky N., Freiman C.J. 1994. Silicone breast implant pathology. Clinical data and immunologic consequences. *Arch. Pathol. Lab. Med.* **118**: 686–693

8. Kossovsky N., Stassi J. 1994. A pathophysiological examination of the biophysics and bioreactivity of silicone breast implants. *Semin. Arthritis Rheum.* **24**: 18–21
9. Luke J.L., Kalasinsky V.F., Turnicky R.P., Centeno J.A., Johnson F.B., Mullick F.G. 1997. Pathological and biophysical findings associated with silicone breast implants: a study of capsular tissues from 86 cases. *Plast. Reconstr. Surg.* **100**: 1558–1565
10. van Diest P.J., Beekman W.H., Hage J.J. 1998. Pathology of silicone leakage from breast implants. *J. Clin. Pathol.* **51**: 493–497
11. Abbondanzo S.L., Young V.L., Wei S., Miller F.W. 1999. Silicone gel-filled breast and testicular implant capsules: a histologic and immunophenotypic study. *Mod. Pathol.* **12**: 706–713
12. Katzin W.E., Feng L.J., Abbuhl M., Klein M.A. 1996. Phenotype of lymphocytes associated with the inflammatory reaction to silicone gel breast implants. *Clin. Diagn. Lab. Immunol.* **3**: 156–161
13. O'Hanlon T.P., Okada S., Love L.A., Dick G., Young V.L., Miller F.W. 1996. Immunohistopathology and T cell receptor gene expression in capsules surrounding silicone breast implants. *Curr. Top. Microbiol. Immunol.* **210**: 237–242
14. Raso D.S., Greene W.B., Vesely J.J., Willingham M.C. 1994. Light microscopy techniques for the demonstration of silicone gel. *Arch. Pathol. Lab. Med.* **118**: 984–987
15. Kidder L.H., Kalasinsky V.F., Luke J.L., Levin I.W., Lewis E.N. 1997. Visualization of silicone gel in human breast tissue using new infrared imaging spectroscopy. *Nat. Med.* **3**: 235–237
16. Naim J.O., Ippolito K.M., van Oss C.J. 1997. Adjuvancy effect of different types of silicone gel. *J. Biomed. Mater. Res.* **37**: 534–538
17. Bar-Meir E., Teuber S.S., Lin H.C., Alosacie I., Goddard G., Terybery J., Barka N., Shen B., Peter J.B., Blank M. 1995. Multiple autoantibodies in patients with silicone breast implants. *J. Autoimmun.* **8**: 267–277
18. Shen G.Q., Ojo-Amaize E.A., Agopian M.S., Peter J.B. 1996. Silicate antibodies in women with silicone breast implants: development of an assay for detection of humoral immunity. *Clin. Diagn. Lab. Immunol.* **3**: 162–166
19. Zandman-Goddard G., Blank M., Ehrenfeld M., Gilburd B., Peter J., Shoenfeld Y. 1999. A comparison of autoantibody production in asymptomatic and symptomatic women with silicone breast implants. *J. Rheumatol.* **26**: 73–77
20. Campbell A., Brautbar N., Vojdani A. 1994. Suppressed natural killer cell activity in patients with silicone breast implants: reversal upon explantation. *Toxicol. Ind. Health* **10**: 149–154
21. Ojo-Amaize E.A., Conte V., Lin H., Brucker R.F., Agopian M.S., Peter J.B. 1994. Silicone-specific blood lymphocyte response in women with silicone breast implants. *Clin. Diagn. Lab. Immunol.* **1**: 689–695
22. Smalley D.L., Shanklin D.R., Hall M.F., Stevens M.V., Hanissian A. 1995. Immunologic stimulation of T lymphocytes by silica after use of silicone mammary implants. *FASEB J.* **9**: 424–427
23. Wilson S.D., Munson A.E. 1996. Silicone-induced modulation of natural killer cell activity. *Curr. Top. Microbiol. Immunol.* **210**: 199–208
24. Ojo-Amaize E.A., Lawless O.J., Peter J.B. 1996. Elevated concentrations of interleukin-1 beta and interleukin-1 receptor antagonist in plasma of women with silicone breast implants. *Clin. Diagn. Lab. Immunol.* **3**: 257–259
25. Ellis T.M., Hardt N.S., Campbell L., Piacentini D.A., Atkinson M.A. 1997. Cellular immune reactivities in women with silicone breast implants: a preliminary investigation. *Ann. Allergy Asthma Immunol.* **79**: 151–154
26. Gutierrez F.J., Espinoza L.R. 1990. Progressive systemic sclerosis complicated by severe hypertension: reversal after silicone implant removal. *Am. J. Med.* **89**: 390–392
27. Spiera H., Kerr L.D. 1993. Scleroderma following silicone implantation: a cumulative experience of 11 cases. *J. Rheumatol.* **20**: 958–961
28. Bridges A.J. 1995. Rheumatic disorders in patients with silicone implants: a critical review. *J. Biomater. Sci. Polym. Ed* **7**: 147–157
29. Meier L.G., Barthel H.R., Seidl C. 1997. Development of polyarthritis after insertion of silicone breast implants followed by remission after implant removal in 2 HLA-identical sisters bearing rheumatoid arthritis susceptibility genes. *J. Rheumatol.* **24**: 1838–1841
30. Beekman W.H., Feitz R., van Diest P.J., Hage J.J. 1997. Migration of silicone through the fibrous capsules of mammary prostheses. *Ann. Plast. Surg.* **38**: 441–445
31. Teuber S.S., Reilly D.A., Howell L., Oide C., Gershwin M.E. 1999. Severe migratory granulomatous reactions to silicone gel in 3 patients. *J. Rheumatol.* **26**: 699–704
32. Posnett D.N. 1995. Environmental and genetic factors shape the human T-cell receptor repertoire. *Ann. N Y Acad. Sci.* **756**: 71–80
33. Steinman L. 1996. A few autoreactive cells in an autoimmune infiltrate control a vast population of nonspecific cells: a tale of smart bombs and the infantry. *Proc. Natl. Acad. Sci. USA* **93**: 2253–2256
34. Offner H., Buenafe A.C., Vainiene M., Celnik B., Weinberg A.D., Gold D.P., Hashim G., Vandenberg A.A. 1993. Where, when, and how to detect biased expression of disease-relevant V beta genes in rats with experimental autoimmune encephalomyelitis. *J. Immunol.* **151**: 506–517
35. Oksenberg J.R., Panzara M.A., Begovich A.B., Mitchell D., Erlich H.A., Murray R.S., Shimonkevitz R., Sherritt M., Rothbard J., Bernard C.A.A., Steinman L. 1993. Selection for T-cell receptor V β -D β -J β gene rearrangements with specificity for a myelin basic protein peptide in brain lesions of multiple sclerosis. *Nature* **362**: 68–70
36. Gold D.P. 1994. TCR V gene usage in autoimmunity. *Curr. Opin. Immunol.* **6**: 907–912
37. Chang J.C.C., Smith L.R., Froning K.J., Schwabe B.J., Laxer J.A., Caralli L.L., Kurland H.H., Karasek M.A., Wilkinson D.I., Carlo D.J., Brostoff S.W. 1994. CD8+T cells in psoriatic lesions preferentially use T-cell receptor V β 3 and/or V β 13.1 genes. *Proc. Natl. Acad. Sci. USA* **91**: 9282–9286
38. O'Hanlon T.P., Miller F.W. 1995. T cell-mediated immune mechanisms in myositis. *Curr. Opin. Rheumatol.* **7**: 503–509
39. Matsumoto I., Tsubota K., Satake Y., Kita Y., Matsumura R., Murata H., Namekawa T., Nishioka K., Iwamoto I., Saitoh Y., Sumida T. 1996. Common T cell receptor clonotype in lacrimal glands and labial

- salivary glands from patients with Sjogren's syndrome. *J. Clin. Invest.* **97**: 1969–1977
40. Kim G., Tanuma N., Kojima T., Kohyama K., Suzuki Y., Kawazoe Y., Matsumoto Y. 1998. CDR3 size spectratyping and sequencing of spectratype-derived TCR of spinal cord T cells in autoimmune encephalomyelitis. *J. Immunol.* **160**: 509–513
41. Striebich C.C., Falta M.T., Wang Y., Bill J., Kotzin B.L. 1998. Selective accumulation of related CD4+T cell clones in the synovial fluid of patients with rheumatoid arthritis. *J. Immunol.* **161**: 4428–4436
42. Davis M.M., Boniface J.J., Reich Z., Lyons D., Hampl J., Arden B., Chien Y. 1998. Ligand recognition by alpha beta T cell receptors. *Annu. Rev. Immunol.* **16**: 523–544
43. Maryanski J.L., Jongeneel C.V., Bucher P., Casanova J.L., Walker P.R. 1996. Single-cell PCR analysis of TCR repertoires selected by antigen in vivo: a high magnitude CD8 response is comprised of very few clones. *Immunity* **4**: 47–55
44. Muraro P.A., Vergelli M., Kalbus M., Banks D.E., Nagle J.W., Tranquill L.R., Nepom G.T., Biddison W.E., McFarland H.F., Martin R. 1997. Immunodominance of a low-affinity major histocompatibility complex-binding myelin basic protein epitope (residues 111–129) in HLA-DR4 (B1*0401) subjects is associated with a restricted T cell receptor repertoire. *J. Clin. Invest.* **100**: 339–349
45. Gown A.M., de Wever N., Battifora H. 1993. Microwave-based antigenic unmasking: a revolutionary new technique for routine immunohistochemistry. *Appl. Immunohistochem.* **1**: 256–266
46. Taylor C.R., Shi S.R., Chen C., Young L., Young C., Cote R.J. 1996. Comparative study of antigen retrieval heating methods: microwave, microwave and pressure cooker, autoclave, and steamer. *Biotech. Histochem.* **71**: 263–270
47. Panzara M.A., Gussoni E., Steinman L., Oksenberg J.R. 1992. Analysis of the T cell repertoire using the PCR and specific oligonucleotide primers. *Biotechniques* **12**: 728–735
48. Maslanka K., Piatek T., Gorski J., Yassai M. 1995. Molecular analysis of T cell repertoires. Spectratypes generated by multiplex polymerase chain reaction and evaluated by radioactivity or fluorescence. *Hum. Immunol.* **44**: 28–34
49. Williams A.F., Strominger J.L., Bell J., Mak T.W., Kappler J., Marrack P., Arden B., Lefranc M.P., Hood L., Tonegawa S., Davis M. 1995. Nomenclature for T-cell receptor (TCR) gene segments of the immune system. WHO-IUIS Nomenclature Sub-Committee on TCR Designation. *Immunogenetics* **42**: 451–453
50. Currier J.R., Yassai M., Robinson M.A., Gorski J. 1996. Molecular defects in TCRBV genes preclude thymic selection and limit the expressed TCR repertoire. *J. Immunol.* **157**: 170–175
51. O'Hanlon T.P., Dalakas M.C., Plotz P.H., Miller F.W. 1994. Predominant TCR- $\alpha\beta$ variable and joining gene expression by muscle-infiltrating lymphocytes in the idiopathic inflammatory myopathies. *J. Immunol.* **152**: 2569–2576
52. Caspi R.R., Chan C.C., Fujino Y., Najafian F., Grover S., Hansen C.T., Wilder R.L. 1993. Recruitment of antigen-nonspecific cells plays a pivotal role in the pathogenesis of a T cell-mediated organ-specific autoimmune disease, experimental autoimmune uveoretinitis. *J. Neuroimmunol.* **47**: 177–188
53. Brown S.L., Silverman B.G., Berg W.A. 1997. Rupture of silicone-gel breast implants: causes, sequelae, and diagnosis. *Lancet* **350**: 1531–1537
54. Beekman W.H., Feitz R., Hage J.J., Mulder J.W. 1997. Life span of silicone gel-filled mammary prostheses. *Plast. Reconstr. Surg.* **100**: 1723–1726
55. Lehmann P.V., Forsthuber T., Miller A., Sercarz E.E. 1992. Spreading of T-cell autoimmunity to cryptic determinants of an autoantigen. *Nature* **358**: 155–157
56. Warnock M.G., Goodacre J.A. 1997. Cryptic T-cell epitopes and their role in the pathogenesis of autoimmune diseases. *Br. J. Rheumatol.* **36**: 1144–1150
57. Rowley M.J., Cook A.D., Teuber S.S., Gershwin M.E. 1994. Antibodies to collagen: comparative epitope mapping in women with silicone breast implants, systemic lupus erythematosus and rheumatoid arthritis. *J. Autoimmun.* **7**: 775–789
58. Young V.L., Nemecek J.R., Schwartz B.D., Phelan D.L., Schorr M.W. 1995. HLA typing in women with breast implants. *Plast. Reconstr. Surg.* **96**: 1497–1519
59. Morse J.H., Fotino M., Zhang Y., Flaster E.R., Peebles C.L., Spiera H. 1995. Position 26 of the first domain of the HLA-DQB1 allele in post-silicone implant scleroderma. *J. Rheumatol.* **22**: 1872–1875